



An investigation of the effect of drawdown pressure on sand production in an Iranian oilfield using a hybrid numerical modeling approach

Nemat Nemati¹ · Kaveh Ahangari¹ · Kamran Goshtasbi² · Reza Shirinabadi^{3,4}

Received: 1 September 2023 / Accepted: 8 January 2024 / Published online: 2 February 2024
© The Author(s) 2024

Abstract

Reservoir pressure reduction due to continuous production from oil and gas wells affects the sand production rate. An increase in drawdown pressure and/or a decrease in reservoir pressure increases the sand production rate. Since the problem of sand production is one of the main issues in the Asmari sandstone formation located in one of the oilfields in the southwest of Iran, therefore, in this research, the variations in the sand production rate due to the changes in the reservoir and drawdown pressures were investigated. So, for the first time, a hybrid numerical model of finite difference method (FDM)—discrete element method (DEM)—finite element method (FEM)—computational fluid dynamics (CFD) was developed. This numerical model investigated the increase in the sand production rate due to variations in reservoir pressure with a constant bottom-hole flowing pressure. Then, by performing an extensive sensitivity analysis on different values of reservoir pressure and drawdown pressure, the changes in the sanding rate, the critical drawdown pressure, and the safe drawdown line were determined. The results showed that, if the production flow rate of the well is constant, increasing the drawdown pressure can change the sand production rate only to a certain extent, and more than that, will be produced at a constant rate. Also, adjusting the drawdown pressure within a safe range does not necessarily keep the sand production rate constant at a permissible value for a long time, while by keeping the bottom hole flowing pressure constant within an acceptable range, the sand production rate can be controlled for a longer period.

Keywords Sand production · Bottom hole flowing pressure · Reservoir pressure · Critical drawdown pressure · Numerical modeling · Safe drawdown line

List of symbols

A_i	Area of each flow element (m^2)
C_{cement}	Cohesion strength of cement between particles (matrix) (MPa)
C_r	Cohesion strength of rock (MPa)
E_c	Young's modulus of casing (GPa)

E_{cement}	Young's modulus of cement between particles (GPa)
E_r	Young's modulus of rock (GPa)
G	Shear modulus of rock (GPa)
K	Bulk modulus of rock (GPa)
K_{cement}	Normal to shear stiffness ratio of cement between particles
N_i	Total number of flow elements
n	Porosity of rock
∇P	Fluid pressure gradient (Pa/m)
Q_t	Total flow rate of the wellbore (m^3/s)
V_i	Fluid velocity in each flow element (m/s)

✉ Kaveh Ahangari
kaveh.ahangari@gmail.com

¹ Department of Mining Engineering, Science and Research Branch, Islamic Azad University, Tehran, Iran

² Department of Mining Engineering, Faculty of Engineering, Tarbiat Modares University, Tehran, Iran

³ Department of Petroleum and Mining Engineering, South Tehran Branch, Islamic Azad University, Tehran, Iran

⁴ Research Center for Modeling and Optimization in Science and Engineering, South Tehran Branch, Islamic Azad University, Tehran, Iran

Greek letters

μ	Friction coefficient of cement between particles
μ_f	Viscosity of the fluid (Pa s)
ν_c	Poisson's ratio of casing
ρ_c	Density of casing (kg/m^3)
ρ_f	Density of the fluid (kg/m^3)
ρ_r	Density of rock (kg/m^3)

σ_H	Maximum horizontal stress (MPa)
σ_h	Minimum horizontal stress (MPa)
σ_t	Tensile strength (MPa)
σ_v	Vertical stress (MPa)
φ_{cement}	Friction angle of cement between particles (°)
φ_r	Friction angle of rock (°)

Acronyms

BHFP	Bottom Hole Flowing Pressure
CDDP	Critical Drawdown Pressure
CFD	Computational Fluid Dynamics
DDP	Drawdown Pressure
DEM	Discrete Element Method
FDM	Finite Difference Method
FEM	Finite Element Method

Introduction

Several factors play a role in controlling the production of sand in oil and gas wells, among which drawdown pressure can be mentioned. The drawdown pressure (DDP) is the difference between the reservoir pressure and the bottom hole flowing pressure (Willson et al. 2002; Fjær et al. 2008; Sun et al. 2021). A decrease in reservoir pressure or an increase in drawdown pressure can increase the amount of sand produced in the well. The main causes of sand production are shear failure caused by mechanical forces and tensile failure caused by drag forces resulting from fluid flow (Papamichos and Stavropoulou 1998; Papamichos et al. 2001; Eshiet and Sheng 2013). On the other hand, considering that changes in drawdown pressure and pore pressure gradient can cause shear failure and tensile failure around wells and perforations, it can be said that changes in drawdown pressure can directly affect the intensity of sand production (Fjær et al. 2008).

The amount of drawdown pressure at which the well starts to produce sand is called critical drawdown pressure (CDDP). So, failure is also related to drawdown pressure at the wellbore and the CDDP parameter needs to be considered by operational engineers. Today, many studies have been conducted on the effect of drawdown pressure on sand control, including analytical, laboratory, and numerical studies. Ghalambor et al. (1989), Willson et al. (2002), Almedej and Algharaib (2005), Rahman and Rahman (2012), Zhang et al. (2016), Oladoyin et al. (2018), Gwamba et al. (2022), and Yosif and Al-Sudani (2022) studies can be mentioned among the analytical and laboratory methods carried out.

The research of Ghalambor et al. (1989), is one of the analytical studies conducted to investigate the effect of drawdown pressure on sand production. Using an analytical model based on Mohr–Coulomb–Navier criteria, they were able to predict sand production in free-water gas wells

located on the U.S. Gulf Coast or similar formations. Morita et al. (1989b) using a simple analytical solution, investigated the effect of drawdown pressure and local pressure gradient around the cavities on the stability of perforations and subsequently sand production. Several analytical studies, including Ghalambor et al. (1994), Weingarten and Perkins, (1995), Ramos et al. (1999), and Vásquez et al. (1999), have examined the impact of drawdown pressure on sand production. Willson et al. (2002), presented an analytical method to determine the critical bottom hole pressure. This geomechanical method is based on the relationship between the effective tangential stress and the effective strength of the formation (which is dependent on the unconfined compressive strength of the reservoir rock samples). So far, many researchers have used this analytical method to determine CDDP (Kasim et al. 2008; Dung and Tung 2014; Subbiah et al. 2014; Pham 2017; Nguyen and Bui 2021; Issa et al. 2022). This method is very simple, it does not require complicated modeling, and the results of this method can be obtained in a shorter time. However, because the unconfined compressive strength is often measured in laboratory conditions and is different from the actual conditions of the reservoir, the obtained results are not reliable. Also, in this method, important and effective parameters in the sand production process, such as the inclination of the well and perforations, the type of the wellbore completion (open hole or cased hole), and the alignment of the well and perforations concerning the in-situ stresses, have not been taken into account.

Numerical modeling is also one of the other methods for the prediction of the CDDP. Until now, many continuum-based numerical models have been presented in this regard (Morita et al. 1989a; Vaziri et al. 2002, 2008; Nouri et al. 2003, 2006a, 2006b; Detournay 2008; Younessi et al. 2013; Hussein and Ni 2018; Li et al. 2018; Eshiet et al. 2019; Zalakinezhad and Jamshidi 2021; Lu et al. 2021). Some of the numerical models made are not at the scale of the well and only a section of that is modeled (axial symmetry). Therefore, the results obtained from these models are not real and only have a study aspect. On the other hand, since the sand production process has a discontinuous nature, in this regard, continuum-based models cannot simulate the real conditions of the well and reservoir. Also, a numerical model based on discontinuum that can investigate CDDP in different states and at the wellbore scale has not been presented.

Since numerical models effectively simulate and describe geomechanical processes, a large-scale numerical model of wells and reservoirs is necessary for modeling sand production. This article presents a new numerical model that has been developed to study the process of sand production in oil fields. This model aims to improve the similarity of numerical models with the complex conditions of the

reservoir and well, particularly when investigating the sand production process in wells with cased-hole completion and perforations. This 3D model is the first to consider certain features (such as wellbore structure, number and arrangement of perforations, fluid flow from the reservoir to the perforations and from the perforations into the well, etc.) not previously accounted for in numerical models investigating sand production. Also, the new FDM-DEM-FEM-CFD hybrid numerical model introduced in this research has been used to investigate the variations in the sand production rate due to drawdown pressure changes in one of the oil fields in southwest Iran.

Hybrid numerical model description

Numerical model selection

In this research, a finite difference model has been used to simulate the reservoir and wall of the wellbore. The program used in this method is FLAC3D software (Itasca Consulting Group Inc. 2021). Due to the complex structure of the well and perforations, it is impossible or very difficult to model these structures with finite difference meshing. Therefore, the meshing of finite elements is coupled in the finite difference model to construct the initial numerical hybrid of FDM-FEM. On the other hand, to more realistically simulate the sand production process, the reservoir structure should be modeled in a discontinuum-based medium. Based on this, PFC3D software (Itasca Consulting Group Inc. 2019) has been used. Constructing a granular medium on the scale of a well and reservoir requires the creation of fine particles in a very large volume, which will increase the number of calculations and consequently slow down the processing speed of the system. For this purpose, a part of the well and reservoir (sanding zone) is modeled in PFC3D and embedded in the FDM-FEM model (which has already been made).

By creating this FDM-DEM-FEM model, in addition to creating a model with the real scale of the well and reservoir, by reducing the volume of modeled particles in the discontinuum medium, the speed of system analysis will also increase. It should be noted that in this modeling, the entire process of sand production is simulated in the PFC3D model.

Layout of the model

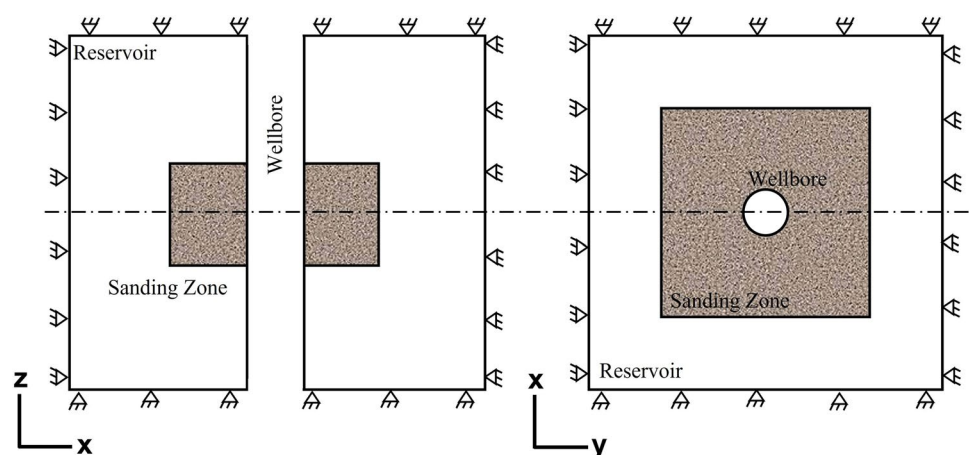
In this modeling, the length, width, and height of the continuum-based model (FDM-FEM) are equal to $2.5\text{ m} \times 2.5\text{ m} \times 2.0\text{ m}$, respectively. The dimensions of the discontinuum medium (located in the middle of the continuum-based model) are also 1.0 m (length) $\times 1.0\text{ m}$ (width) $\times 0.5\text{ m}$ (height). The depth (length) and width of the wellbore are 2.0 m and 0.1397 m , respectively. In this modeling, a hollow cylinder has been made as a casing with a length of 2.0 m , a thickness of 3.0 cm , and an inner diameter of 0.216 m . Therefore, the radius of the wellbore with the casing is 0.10795 m .

The values related to the physical characteristics and mechanical parameters of the casing are considered based on the standards of the American Petroleum Institute (API) (API 2012; Hansen 2018). A simple plan of the initial structure of the model can be seen in Fig. 1.

820,450 spherical particles with a diameter of 0.5 to 7.0 mm are randomly placed throughout the discontinuum model. Those number of FLAC3D zones that interface with the particles is considered PFC3D walls. In terms of mechanical behavior, these walls follow FLAC3D zones, and accordingly, the forces acting on the FLAC3D zones and displacements are easily transferred to the PFC3D particles.

The contact model that is considered for the connection of particles is the flat-joint model. By using this contact model, the structure of the material is preserved during the failure and it is possible to observe the changes in the damaged area at any moment of the failure process (Potyondy

Fig. 1 Schematic of the geometry of a wellbore, sanding zone, and reservoir in the hybrid numerical model



and Mas Ivars 2020). Also, there have been reforms that have increased the advantage of using this contact model, compared to similar models before it (Potyondy and Cundall 2004). The description, formulation, and other characteristics of the flat-joint model are given in studies by Potyondy and Cundall (2004), Potyondy (2018), Potyondy (2019), and Potyondy et al. (2020).

Initial and boundary conditions of the model

In this numerical model, the grid points located in the corners, edges, and outer boundaries of the finite difference model are considered fixed, and in-situ stresses are also applied to the model. Also, a cylindrical area around the casing with a radius of 20.0 cm is considered the cement sheath around the wellbore and is fixed. Several horizontal cylinders with 0.01 m in diameter and 0.30 m in length near the wellbore wall in the PFC3D model, and several holes with 0.01 m in diameter on the casing, are created as perforations. Also, in this model, the casing and cemented layer are considered fixed. The final state of the constructed hybrid model of the wellbore can be seen in Fig. 2.

Model verification

In this research, to validate the DEM model, the analytical solution of Risnes et al. (1982) has been used. Assuming axial symmetry and plane strain conditions and using the Mohr–Coulomb criterion, they obtained analytical solutions for stress distribution around the wellbore. The details and formulation of this analytical solution are found in Risnes et al. (1982) and Cui et al. (2016).

Using some hypothetical data, the sanding zone is constructed in PFC3D and then it is loaded with an arbitrary boundary stress of 35.0 MPa. After running the program, the analysis process continues until the intensity of unbalanced forces reaches less than 1.0×10^{-4} times the contact forces. By measuring the average stress in the PFC3D model, radial

and tangential stresses are determined. Also, the radius of the plastic zone is determined by measuring the distance between the well wall and the position where the tangential stress reaches its maximum value. Then, with the previous hypothetical data, an analytical model is created using the Risnes solution. Figure 3 shows the results of the Risnes analytical method and the DEM numerical model. According to this figure, the radial stress and tangential stress diagrams obtained from both analytical and numerical methods have converged toward the value of 35.0 MPa. This value is the confining pressure applied to the external boundaries of the DEM model. As can be seen in the figure, there is a difference between the peak values of the tangential stress measured in the analytical solution and the numerical method, which can be partly due to the averaging method of the DEM model in calculating stresses (Climent et al. 2013, 2014).

Fluid flow modeling

In this modeling, computational fluid dynamics (CFD) has been used to simulate the fluid flow in the sand production process. This computational method investigates the fluid-particle interaction in a DEM medium. CFD usually considers the nonlinear flow equations in an iterative manner in a finite element model. Details and formulations of fluid-particle interaction in a CFD-DEM model are given in Tsuji et al. (1993).

Since to define the fluid flow in the CFD model, separate elements and meshing are needed, the elements of the flow must be designed in such a way that it simulates the conditions of fluid movement from the reservoir to the wellbore. Considering that in real field conditions, the fluid enters the well through perforations, the flow elements must be aligned with the perforations that are modeled in the casing wall. In this research, finite element meshing has been used to simulate fluid flow. In the design of the CFD model, the dimensions of the flow elements should be selected in such a

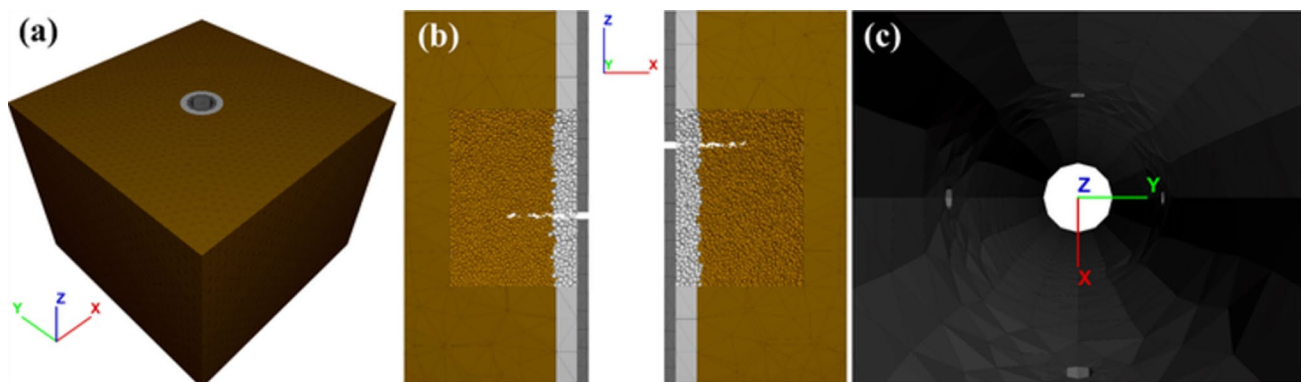
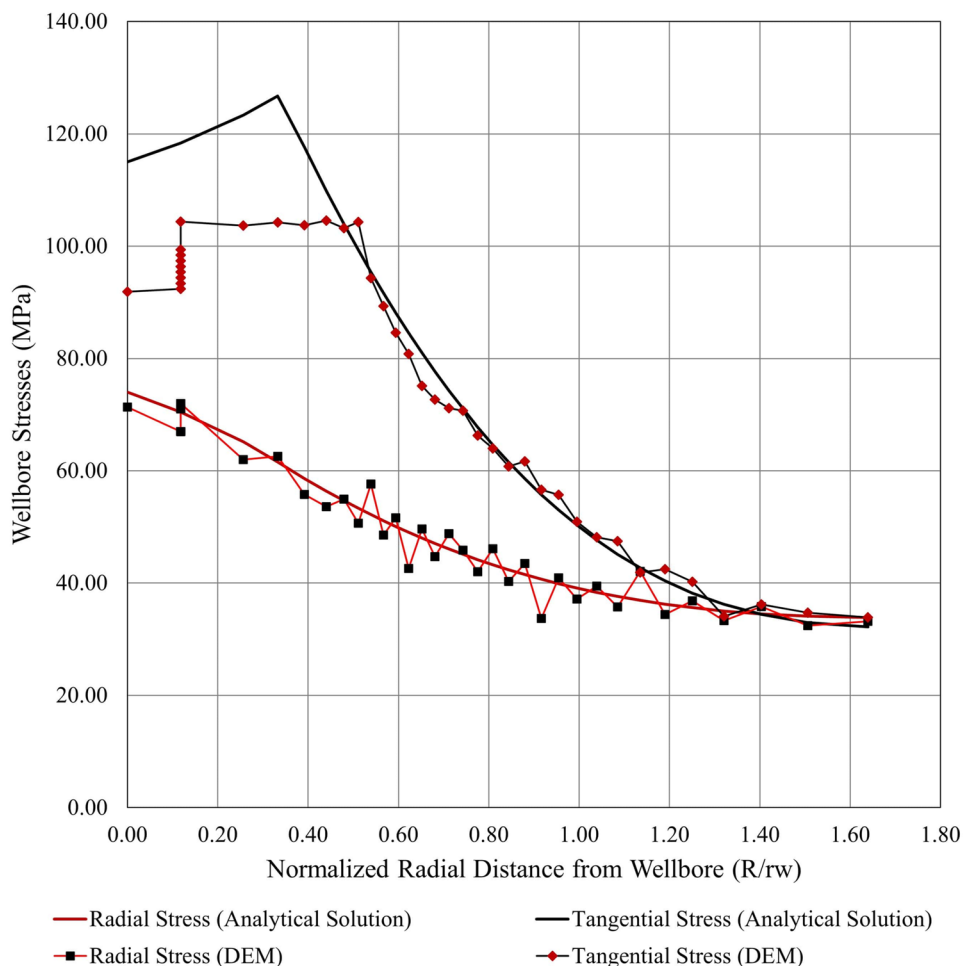


Fig. 2 Configuration of the model: **a** 3D view of the model, **b** Cross section of the model, and **c** Perforations that have been created in the casing

Fig. 3 The results of the Risnes analytical solution and DEM method in measuring radial and tangential stresses



way that the size of the smallest element is larger than that of the largest particle modeled in PFC3D. A fluid-related body force is applied, on average, to a fluid element. The force applied on the particles by the fluid is also exerted locally by the flow element occupied by the particle. Porosity and drag force are calculated as an average of particle properties in each fluid element (Itasca Consulting Group Inc. 2021).

The CFD module is utilized to simulate the fluid flow in the PFC3D, and Python 3.6, which has been particularly configured for utilization in Itasca software, is used as the CFD solver. The elements of fluid flow that have been used in this modeling, with the direction of fluid movement into the well are shown in Fig. 4.

Applying reservoir and bottom hole pressures to the model

In this numerical model, the designed CFD model is not able to simulate the reservoir and bottom hole pressures. For example, in the well model with cased hole completion, there is only a limited flow along the perforations, which only simulates the fluid flow, and it cannot affect

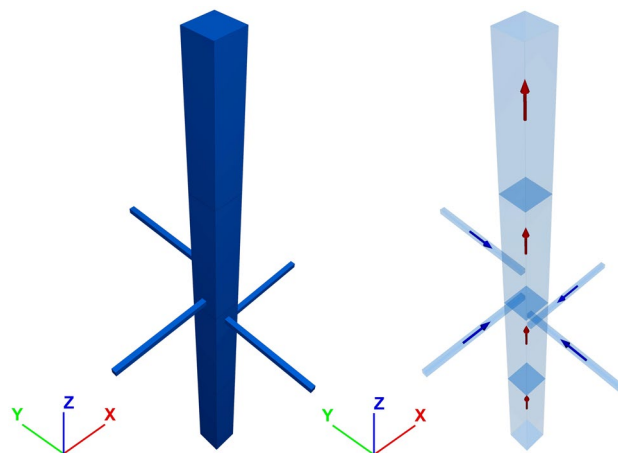


Fig. 4 CFD elements and the direction of fluid flow in a vertical well (the fluid moves from perforations into the wellbore)

the model as reservoir pressure. Therefore, to model reservoir pressure and bottom hole pressure, new forces are needed that must be applied to the PFC3D particles. To simulate the reservoir pressure to the models, a contact

force is applied radially from the outermost points of the discontinuum model (i.e., the border of the PFC3D and FLAC3D models) towards the center of the wellbore. So that this force can surround all the contacts of the particles in the model and affect them. In other words, a new contact force is added to the previous forces of the model, and the algebraic sum of this new contact force divided by the area of the model that is affected by it will be equivalent to the reservoir pressure in that area.

The same method is also used for applying wellbore pressure to the model. That is, from the side of the wall of the wellbore, a force is applied to the contact of the particles located around the well, and the sum of these forces in those areas is equivalent to the bottom hole pressure. The application of this contact force by a hypothetical well to the particles around it is shown in Fig. 5a and the displacement vectors of the particles around a well after applying reservoir pressure and bottom hole pressure are shown in Fig. 5b.

Kessler et al. (1993), in their pseudo-3D model, considered the pressure of a well with cased hole completion to be approximately equal to mud pressure (before wellbore completion) or cementation pressure (during wellbore completion and assuming a perfect cementation job). Therefore, in this research, for the models, the mud pressure is considered as the wellbore pressure. Because: (1) In this model, the casing and the cemented layer around it are fixed. Therefore, they cannot apply any forces to the space around them, and (2) information about the completion and cementing operations of the wellbores located in the studied oil field (such as cement quality, cementing pressure, etc.) was not available to the authors. The final state of a hypothetical well, after drilling and before completion, is shown in Fig. 6. This vertical well has reached mechanical equilibrium after being subjected to the in-situ stresses, reservoir pressure, and bottom hole pressure.

Fig. 5 **a** Simulation of the pressure of a hypothetical well on the particles around it, and **b** The displacement vectors of particles around a hypothetical well, due to the application of reservoir pressure, bottom hole pressure, and field stresses in the DEM model

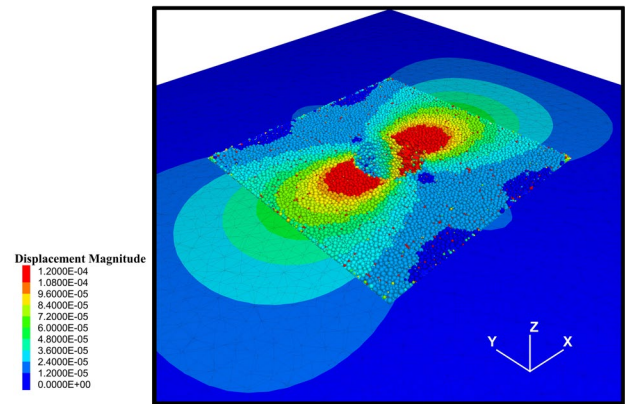
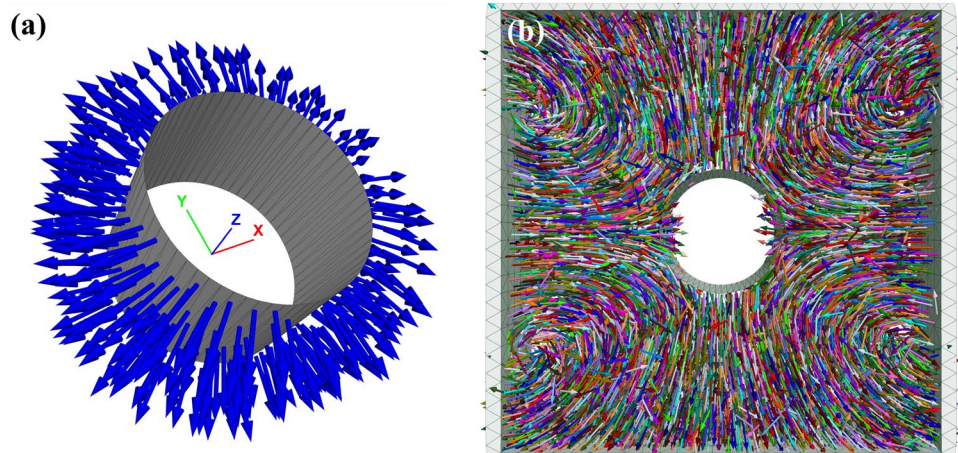


Fig. 6 Displacement curves around a hypothetical well after drilling and before completion that is affected by field stresses, reservoir pressure, and bottom hole pressure

Simulation of the sand production process

Once the initial geometry of the model is constructed and the initial and boundary conditions are applied, the model undergoes mechanical analysis until the applied forces reach mechanical equilibrium. In the next step, the fluid flow is included in the model. For this purpose, the velocity of the fluid needs to be specified for the CFD elements. With the knowledge that the production flow rate of the well is directly related to the fluid velocity, and with the assumption that the fluid velocity is the same in all perforations, Eq. (1) can be used to determine the fluid flow rate through each element at each time step.

$$V_i = \frac{Q_t}{A_i \times N_i} \quad (1)$$

where V_i (m/s) is the fluid velocity in each flow element, Q_t (m^3/s) is the total flow rate of the wellbore (it is determined

based on the flow rate of the well), A_i (m^2) is the area of each element of the flow, and N_i (dimensionless) is the total number of flow elements. Once the velocity of the fluid flow has been calculated and applied to the model, certain particles can not withstand the mechanical loads and hydrodynamical forces caused by the fluid flow. These degraded particles become dislodged from their position and are carried into the wellbore by the fluid. A set of points within the well, specifically at the center of the perforations, is defined by the user. These points are used to measure the mass of particles passing through them at any moment during the analysis process. The amount of mass of particles passing through the perforations in each time step is called the instantaneous production of sand. The cumulative sand production is obtained from the sum of instantaneous sand production values in a certain period. The cumulative production of sand, divided by the volume of fluid passing through the perforations at any time, gives the sand production rate at that time. The program can also generate diagrams showing the instantaneous sand production, cumulative sand production, and sand production rate for each time step. Figure 7 shows the situation of a hypothetical well after the application of in-situ stresses, reservoir pressure, bottom-hole flowing pressure, and fluid flow, and the graph in Fig. 8 illustrates the sand production rate for a wellbore using hypothetical data.

During the stage of fluid production and sand erosion, the analysis will continue until either no more sand is produced or the sand production rate becomes constant. When such a situation is reached, the analysis will come to a halt. It takes approximately 600s (or 150,000 cycles) for the sand production rate graph to stabilize at a constant value in this

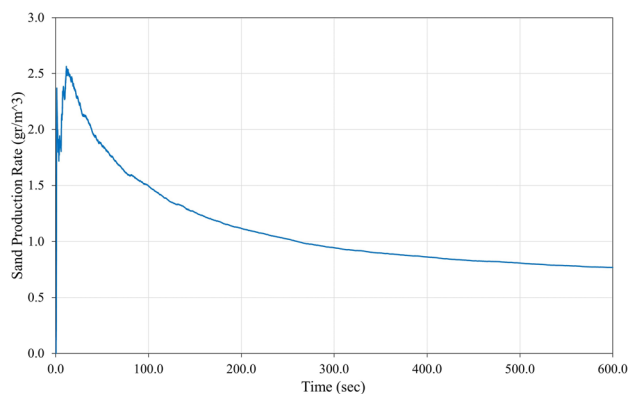


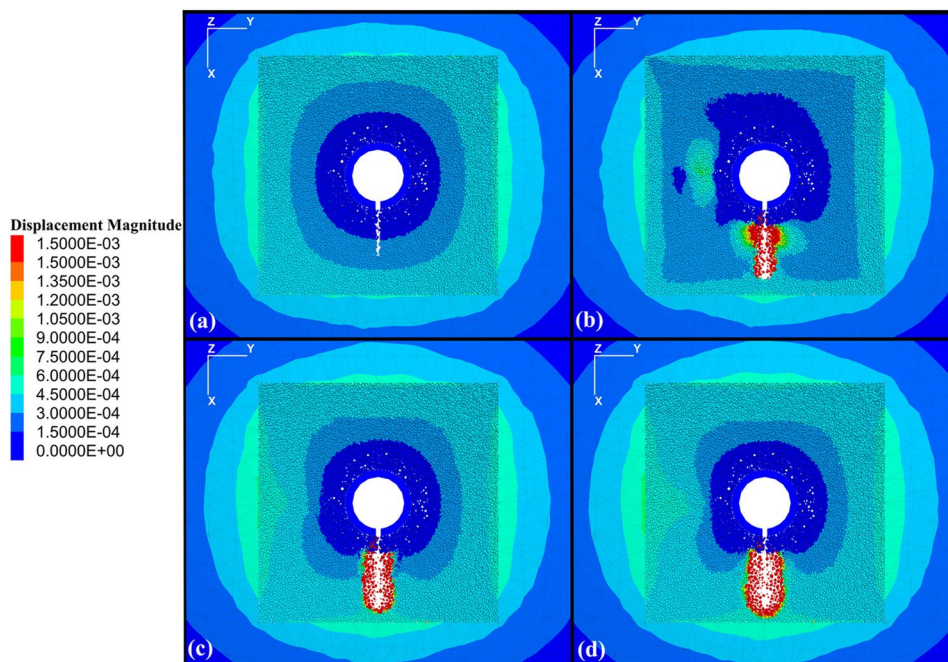
Fig. 8 Sand production rate versus time for a hypothetical well with a production flow rate of 1500 bbl/day which is calculated by the model

simulation. See Fig. 8 for an example. This scenario can be seen in almost all models. On a PC with an Intel Core CPU running at 3.7–4.5 GHz, simulating the sand production process for one minute takes approximately 8 h. Therefore, running each model, which consists of 150,000 cycles, will require a total of 80 h.

Case study

The oil field studied in this research is located in southwest Iran. This is located in an anticline with a gentle NE-SE trend. This anticline is part of a wide fold with the NW-SE direction (Abdollahie Fard et al. 2006). This structure belongs to the stable shelf of the Arabian platform and

Fig. 7 Horizontal section of a vertical wellbore model with hypothetical data, affected by field stress, reservoir pressure, and BHFP: **a** before applying fluid flow, **b** after 30,000 cycles, **c** after 60,000 cycles, and **d** after 150,000 cycles of applying fluid flow, with a flow rate of 2000 bbl/day



only limited outcrops of it are on the surface. Therefore, it is difficult to perform detailed geological evaluations of these outcrops. This field is one of the rich oil systems in the Middle East that includes Gurpi, Kazhdumi, and Gadvan source rocks and Asmari, Fahlyan, and Kazhdumi/Bangestan reservoirs. Field data obtained from this structure show unconformable and eroded surfaces. This can be due to the uplifting of the basement horsts (Berberian 1995).

Because the studied reservoir in this oil field is located in the Asmari formation, it is known as the Asmari reservoir, and it consists of alternate layers of dolomite, limestone, anhydrite, sandstone, and shale. Generally, in the sedimentary environments of southwest Iran, sandstones are divided into lower parts (Eocene–Oligocene) and upper parts (Early Miocene). At the end of the Oligocene and the border of the Miocene, shallow carbonate environments, most of which are in the Zagros basin, covered that area. This carbonate environment penetrated from the northern regions of the Persian Gulf to the southwestern regions of Iran with sand and limestones that are located in depth and formed the carbonate and sandstone reservoirs of Iran (Alavi 2004).

The oil producer of the Asmari reservoir in this oil field is mainly sandstone. Based on research, the quality of sandstone in this formation decreases significantly with increasing depth. Accordingly, the exploitation of this oil field is associated with significant sand production. So, oil companies have to spend a lot of money every year to control the sand and compensate for the damages caused by the production of sand. Therefore, in this research, by presenting a hybrid numerical model, it is possible to study the sand production process for optimization of production, to reduce the sand production rate of wellbores located in this oil field.

Simulation results and discussions

Calibration of the numerical model with reservoir conditions

Here, to simulate the reservoir conditions in the numerical models, the geomechanical data obtained from well C have been used. Well C is a vertical wellbore that is drilled in the studied oil field. The oil producer layer in this well is layer A10 of the Asmari reservoir, which is located at a depth of 2661 m from the surface. The geomechanical data related to this layer has been obtained through the petrophysical logs measured in well C, and they are listed in Table 1. Table 1 shows the geomechanical information related to layer A10 of the Asmari reservoir after analyzing and converting the dynamic into static parameters through formulas and laboratory tests. According to the operational reports, Well C has a sand production problem, so that with a flow rate of 2000 barrels per day, this well is on the threshold of producing

Table 1 Geomechanical parameters of simulation related to layer A10 in the Asmari Reservoir

	Parameters (Symbol)	Values	Units
Field Stress	Vertical Stress (σ_v)	71.25	MPa
	Maximum Horizontal Stress (σ_H)	53.11	MPa
	Minimum Horizontal Stress (σ_h)	47.42	MPa
Macroscopic	Density of Rock (ρ_r)	2270.0	kg/m ³
	Young's Modulus of Rock (E_r)	9.60	GPa
	Shear Modulus (G)	3.78	GPa
	Bulk Modulus (K)	6.956	GPa
	Tensile Strength (σ_t)	2.30	MPa
	Cohesion Strength (C_c)	5.485	MPa
	Friction Angle (φ_r)	39.0	(°)
	Cohesion of Cement (Matrix) (C_{cement})	21.15	MPa
Microscopic	Friction Coefficient of Cement (μ)	0.1	–
	Friction Angle of Cement (φ_{cement})	34.634	(°)
	Young's Modulus of Cement (E_{cement})	16.14	GPa
	Normal to Shear Stiffness Ratio of Cement (K_{cement})	1.25	–
	Number of Elements	4.0	–
	Casing	Density of Casing (ρ_c)	7850.0
Young's Modulus of Casing (E_c)		210.0	GPa
Poisson's Ratio of Casing (ν_c)		0.3	–
Fluid	Density of the Fluid (ρ_f)	840.0	kg/m ³
	Viscosity of the Fluid (μ_f)	0.006	Pa s
	Porosity (n)	0.23	–
	Fluid Pressure Gradient (∇P)	9.991	Pa/m

sand. Although the amount of sand produced does not cause a problem in the production process of the well, with the increase of the flow to more than 2500 barrels per day, the production of significant amounts of sand disrupts the performance of this well.

According to the data in Table 1 and the modeling procedure in Sect. “Hybrid numerical model description”, a preliminary model of well C is constructed. Four horizontal holes with a radius of 1.0 cm and a length of 30.0 cm are embedded as perforations in the inner wall of the casing, which are spirally arranged at 90° and a vertical distance of 10.0 cm from each other. Since in this modeling, it is assumed that the output fluid flow rate from all perforations is the same, therefore, in selecting the number of perforations, the algebraic sum of the output flow rate of all perforations must be equal to the total flow rate of the well. Also, by CFD elements, the fluid flow in the model of well C is simulated, in such a way that the fluid enters the well through the perforations and then flows to the upper parts. As can be seen in Table 1, the fault regime in layer A10 of the Asmari reservoir is normal. In this reservoir, the direction of minimum horizontal stress is determined as N40W/S40E, according to the breakouts observed by the ultrasonic

borehole imagers. The situation of Well C about the geographical directions and the position of horizontal stresses is shown in Fig. 9. The horizontal stresses are applied to the model in such a way that the minimum horizontal stress is along the X-axis and the maximum horizontal stress is along the Y-axis.

Mohr–Coulomb and elastic criteria have been used for the formation and casing zones in the continuum model, respectively. Also, the flat-joint contact model is chosen to simulate the cement between sandstone particles in the discontinuum model. Since it is not possible to determine the geomechanical parameters of the cement between the reservoir particles in layer A10, through common methods such as logs, therefore, using a methodology, the PFC3D model should be calibrated with the sandstone in layer A10. In this way, the situation of well C is first determined in terms of sand production. Then, by performing a sensitivity analysis on the geomechanical parameters related to the contact of the particles in the model (such as cohesion, friction angle, Young's modulus, etc.) and repeating the analysis process, finally, the obtained sand production rate should be equal to the same amount measured from well C. In this way, the condition of the particles simulated in the numerical model will match with the real conditions of the reservoir in layer A10.

However, since no sand monitoring activity has been carried out in the studied oil field and the amount of sand produced in the wellbores has not been precisely measured, the sand production rate for well C should be approximately estimated. As mentioned above, well C is on the threshold of sand production with a flow rate of 2000 bbl/day. Based on the studies of Ghalambor et al. (1989, 1994) and Veeken et al. (1991), the allowed rate of sand production

in oil-producer wells is equal to 6–600 g/m³ and in gas-producer wells, this value is equal to 16.8 × 10⁻⁶ kg/m³. However, in the studied oil field, due to the specific conditions of the reservoir and the low resistance of the wellbore equipment against solid particles, operational engineers have considered the allowable amount of sand for oil wells to be between 1.0–10.0 ppm (and in critical conditions, a maximum of 15.0 ppm). Considering that the density of sandstone in layer A10 has been measured as 2270 kg/m³, therefore, the allowable rate of sand production in this reservoir is between 2.3 and 34.0 g per cubic meter. Since the main objective in this oil field is to produce the lowest amount of sand along with fluid without installing any mechanical equipment to prevent sand production, such as gravel pack, sand screen, etc., in this research, the maximum allowable rate of sand production is considered as 1.0 g/m³ (0.44 ppm).

Considering that well C produced a small amount of sand with a flow rate of 2000 bbl/day and this amount of sand did not cause any problems in the production process of the well, it is assumed that the sand production rate in well C with a flow rate of 2000 bbl/day is equivalent to 1.0 g per cubic meter. That is, well C with a flow rate of 2000 bbl/day produces 1 g of sand for every cubic meter of crude oil production (regardless of the amount of water produced). By performing sensitivity analysis on different values of geomechanical parameters in the contact model of particles, the wellbore model with a flow rate of 2000 bbl/day is run several times until the final sand production rate in this numerical model is equal to 1.0 g/m³. Figure 10 shows the diagrams of cumulative sand production versus volume of produced fluid and sand production rate versus time for well C after performing sensitivity analysis. As can be seen, the trend of the sand production rate diagram is fixed at 1.0 g/m³. In this way, the numerical model of the particles is calibrated with the conditions of the sandstone in layer A10, and it is proper to be used in reservoir studies. The final values of geomechanical parameters of cement (matrix) related to the sandstone of the Asmari reservoir in layer A10 are given in Table 1. Also, the process of changing the shape of the cavities in well C during analysis can be seen in Fig. 11.

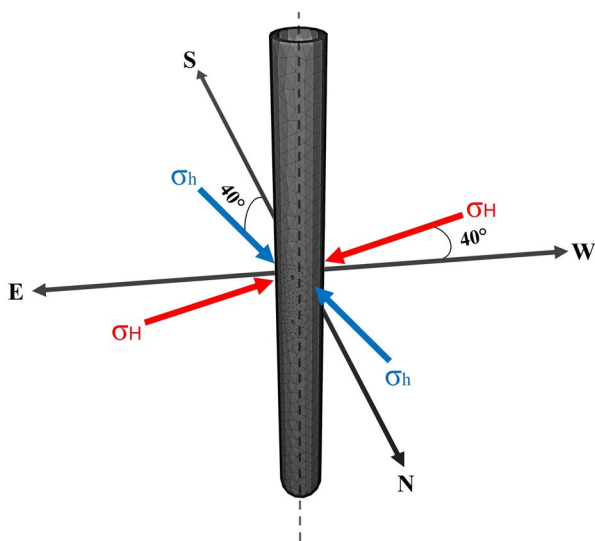


Fig. 9 Schematic of the position of the horizontal stresses relative to well C

Investigation of the effect of DDP variations on sand production rate

To investigate the effect of reservoir pressure changes on the sand production rate in layer A10 of the Asmari formation, the vertical well model calibrated in Sect. “Calibration of the numerical model with reservoir conditions” has been used. This vertical well is subjected to variable reservoir pressures (2000, 2500, 3000, 3500, and 4000 psi) and a constant bottom hole flowing pressure (BHFP) of 1500 psi. Also, the flow rate of the well is considered to be 2000 barrels per day in each situation. After analyzing the

Fig. 10 Sand production rate vs. time and cumulative sand production vs. volume of produced oil in Well C, after the final analysis

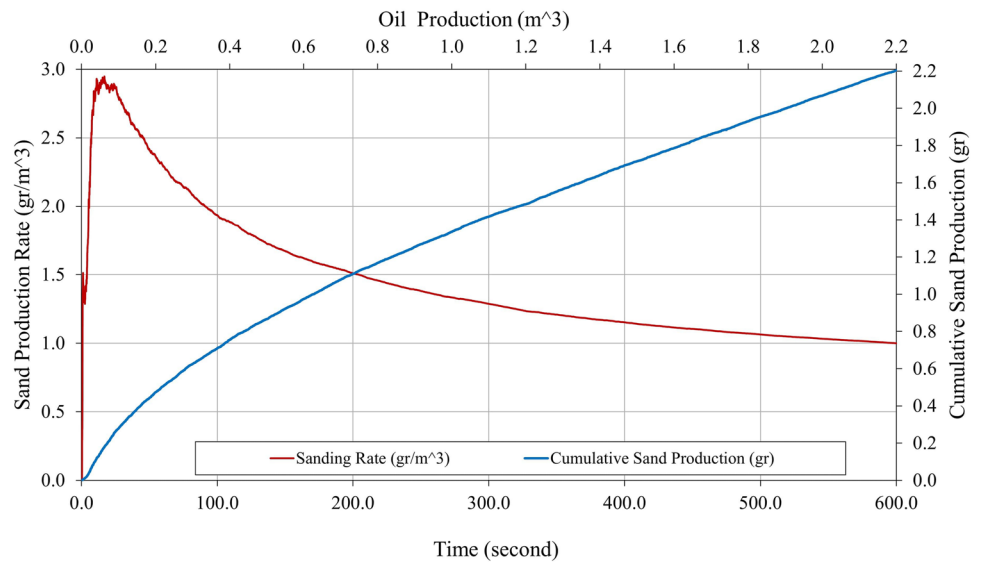
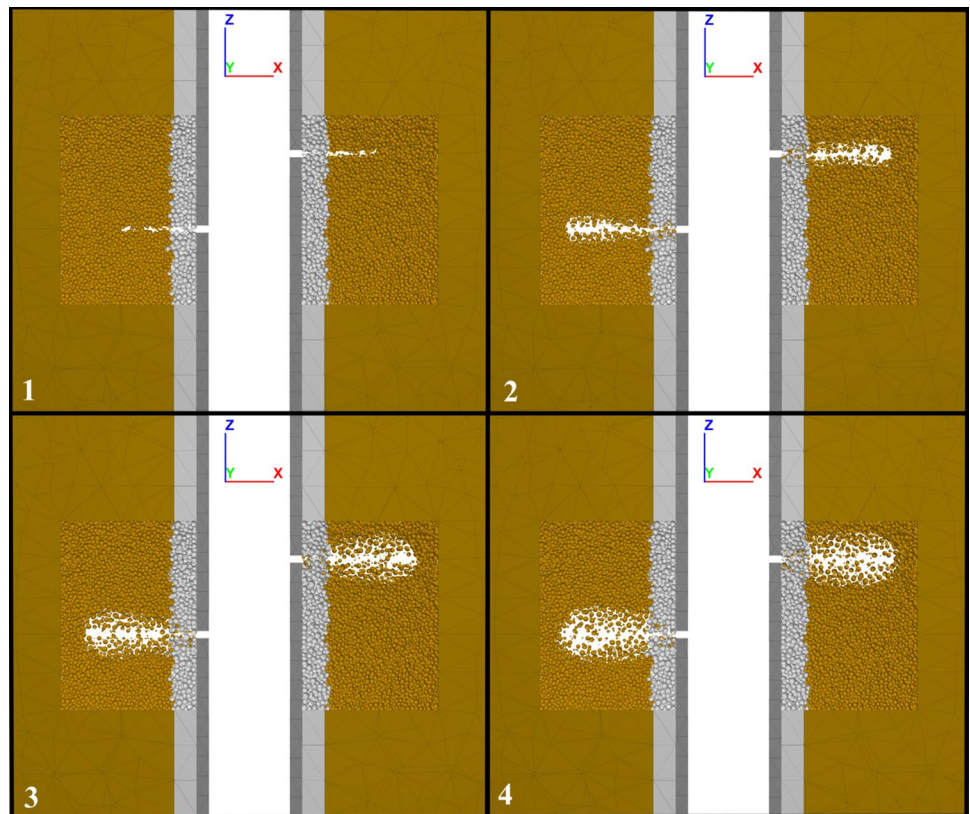


Fig. 11 The gradual deformation of the cavities around well C, due to fluid flow and sand production during analysis



models, the values of cumulative sand production and sand production rate were measured for each mode, and the corresponding diagrams were drawn. These diagrams can be seen in Figs. 12 and 13. As can be seen in the figures, as long as the BHFP is constant, the higher the reservoir pressure, the higher the sand production rate. Also, in Fig. 14, the diagram of sand production rate changes according

to drawdown pressure is shown. According to the figure, in the beginning, the sand production rate diagram has a relatively large gradient. Gradually, with the increase of drawdown pressure, the gradient of the graph decreases, and if the analysis continues up to higher values of the dropdown pressure, the process of changes in the sand production rate may remain constant at a certain value.

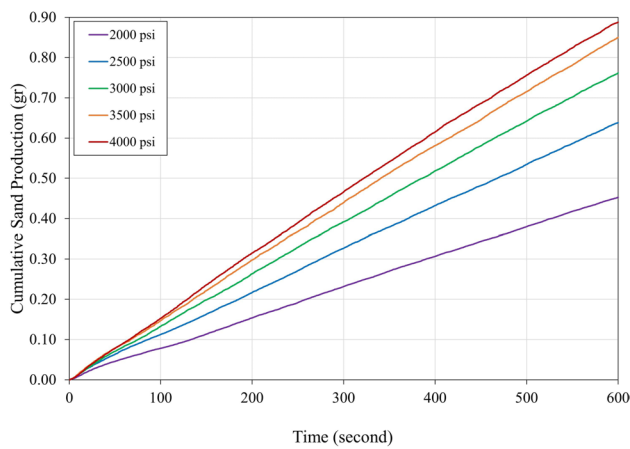


Fig. 12 Cumulative sand production versus time for a vertical wellbore, with different reservoir pressures (BHFP=1500 psi, and production flow rate=2000 bbl/day)

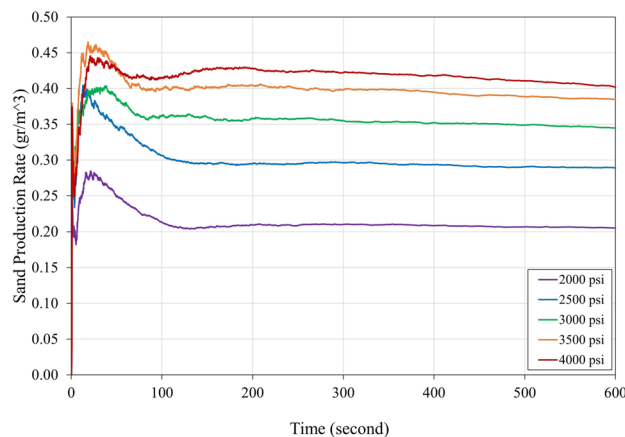


Fig. 13 Sand production rate versus time for a vertical wellbore, with different reservoir pressures (BHFP=1500 psi, and production flow rate=2000 bbl/day)

Determination of critical drawdown pressure in layer A10

To determine the CDDP in a vertical well drilled in layer A10 of the Asmari reservoir, the hybrid numerical modeling introduced in this research has been used. Using extensive sensitivity analysis on different values of reservoir pressure and drawdown pressure in a vertical well (completed with casing and cement sheath) with a flow rate of 2000 bbl/day, the sand production rate corresponding to each situation is measured. Figure 15 shows the results of these sensitivity analyses. As can be seen in this figure, if the reservoir pressure is constant, the sand production rate will also increase in proportion to the increase in the drawdown pressure. If the permissible rate of sand production is considered equal to

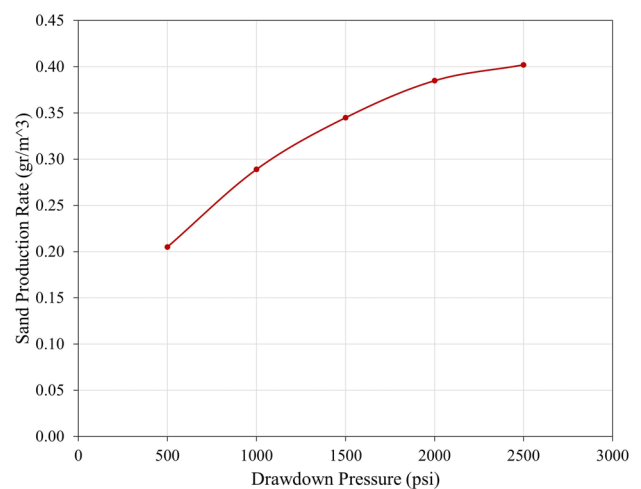


Fig. 14 Sand production rate versus drawdown pressure for a vertical wellbore in layer A10 of Asmari reservoir (BHFP=1500 psi, and production flow rate=2000 bbl/day)

1.0 g/m³ (red dashed line in the figure), the sand production rates above the permissible limit are related to the lower values of the reservoir pressure and drawdown pressure. That is the lower the reservoir pressure values, the higher the sand production rate, and vice versa, the higher the reservoir pressure is, the sand production rate will decrease as the drawdown pressure increases. If the reservoir pressure is high and the BHFP decreases (and as a result, the drawdown pressure increases), the pore pressure around the wellbore increases, which causes the effective stress to decrease. As the effective stress decreases, the stress concentration around the well and perforations will decrease, and with the reduction of the plastic shear strain, the sand production rate is also reduced.

Also, in a situation where the drawdown pressure is constant, the sand production rate will increase with the reduction of the reservoir pressure. For example, in Fig. 15, for a constant drawdown pressure of 1500 psi, there are five different values of sand production rate; So with the reduction of reservoir pressure, the sand production rate increases significantly. This process is also seen in other drawdown pressure values. Therefore, with the drawdown pressure remaining constant at a certain value, the gradual reduction of the reservoir pressure will subsequently increase the sand production rate. The reason for this process is the opposite of the previous situation. That is, with the reduction of reservoir pressure (reduction of pore pressure), the intensity of effective stresses will increase, and as a result, the plastic shear strain in the areas around the wellbore and perforations will increase. This situation will increase the sand production rate over time.

In Fig. 15, the BHFP curves are obtained by connecting the points where the reservoir pressure and drawdown pressure differences are equal. This process can be seen in

Fig. 15 Sand production rate versus drawdown pressure, for different amounts of reservoir pressure in a vertical well with a daily flow rate of 2000 barrels located in layer A10 of the Asmari reservoir

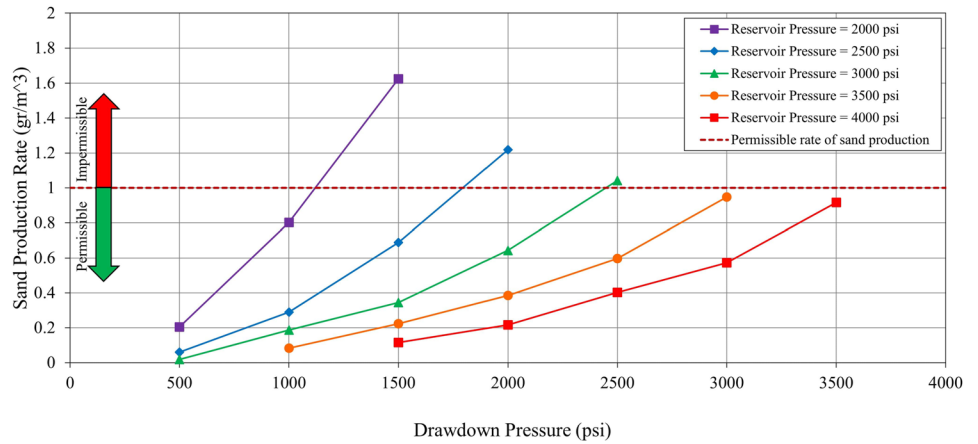


Fig. 16. According to this figure, the sand production rate also increases with the decrease of the BHFP.

According to Fig. 16, if the BHFP is constant (especially at high values), the changes in drawdown pressure will not significantly affect the sand production rate. For example, in the curve corresponding to BHFP equal to 1500 psi, the sand production rate for drawdown pressures of 500 and 2500 psi is 0.205 and 0.402 g/m³, respectively. In other words, when the BHFP is constant at 1500 psi, the difference in the sand production rate due to the decrease in reservoir pressure from 4000 to 2000 psi (or the increase in drawdown pressure from 500 to 2500 psi), will be only 0.197 g/m³. This situation can be seen almost for all other BHFP curves. However, this process is different for reservoir pressure curves. For example, in the reservoir pressure curve of 3500 psi, the sand production rate for a drawdown pressure of 1000 psi is equal to 0.083 g/m³ and for a drawdown pressure of

3000 psi, it is equal to 0.948 g/m³. That is, with the reservoir pressure being constant at 3500 psi, the difference in sand production rate due to drawdown pressure changes from 1000 to 3000 psi is equal to 0.865 g/m³. This value is equal to 1.42 g/m³ for the reservoir pressure curve of 2000 psi, and the pressure drawdown between 500 and 1500 psi. Therefore, in this oilfield, in conditions where the reservoir pressure is constant, BHFP changes have a significant effect on the sand production rate. While if the BHFP is constant (especially for values of 1500 psi and above), changes in the reservoir pressure do not have much effect on increasing the sand production rate.

In Fig. 16, in the BHFP curves with values of 1500, 2000, and 2500 psi, increasing the drawdown pressure has caused a slight increase in the sand production rate. While in the curves related to BHFP with values of 500 and 1000 psi, the increase in pressure drawdown has caused a

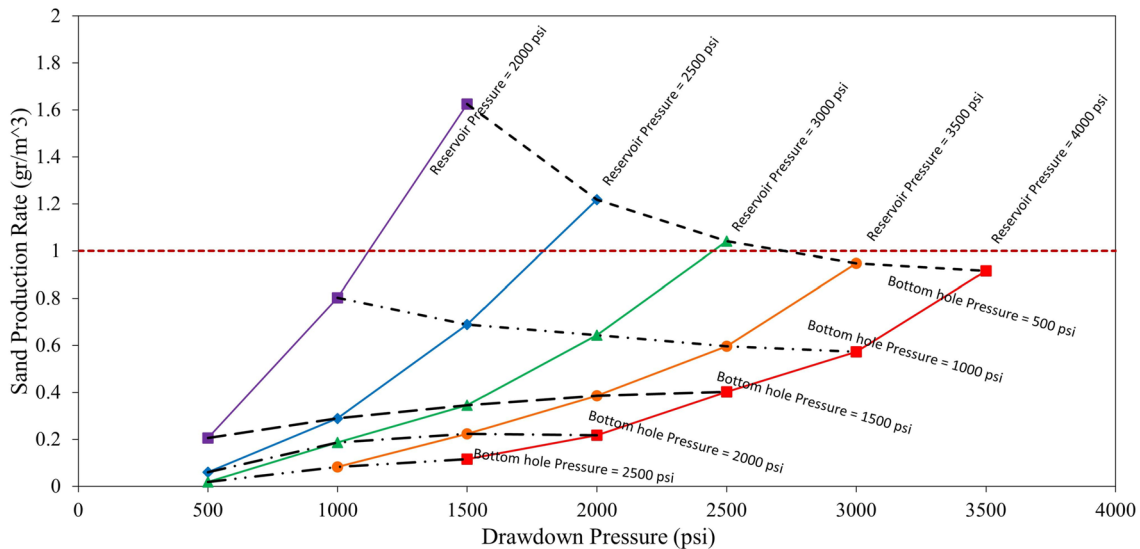


Fig. 16 Creation of BHFP curves, according to different values of sand production rate and reservoir pressure in a vertical well with a flow rate of 2000 bbl/day in layer A10 of Asmari reservoir

gradual decrease in the sand production rate. Therefore, increasing the drawdown pressure for low BHFP values decreases the sand production rate, and for high BHFP values, it increases the sand production rate. Mathematically, this process can be justified in such a way that in situations where the BHFP value is low, drawdown pressure changes depend only on reservoir pressure variations. Under these conditions, the higher the reservoir pressure is, with the increase in pore pressure, the intensity of the effective stresses also decreases, and as a result, it leads to a decrease in the sand production rate. Therefore, the sand production rate in the BHFP curves with values less than 1500 psi has a downward trend. However, in a situation where BHFP increases significantly, in addition to influencing the drawdown pressure, it is also able to control the sand production rate. As can be seen, in the BHFP curves higher than 1500 psi, although the trend of variations in the sand production rate is upward, increasing the BHFP values reduces the sand production rate to an acceptable level.

On the other hand, in all BHFP curves, the sand production rate tends to a constant value in proportion to the increase in drawdown pressure. This means that with a constant BHFP, increasing the drawdown pressure only up to a specific value can increase or decrease the sand production rate, and from that value onward, with the increase of drawdown pressure, the trend of changes in the sand production rate will be fixed. Perhaps the reason is the direct relationship of BHFP with the ability to transport solid particles by fluid flow to the upper parts of the well. That is, as long as the BHFP is constant, the fluid flow can carry a certain amount of sand particles to the higher parts of the wellbore,

and this value fluctuates according to the reservoir pressure and wellhead flowing pressure variations.

Therefore, the drawdown pressure (difference between reservoir pressure and BHFP) must be kept constant in such a way that in addition to increasing the production efficiency of the wellbore, it is possible to simultaneously bring the sand production rate to the lowest value. In Fig. 17, assuming that the allowable sand production rate in a vertical well with a flow rate of 2000 bbl/day is equal to 1.0 g/m^3 , the values of reservoir pressure and drawdown pressure under which the sand production rate exceeds the allowable limit are shown in red. So, in this well, according to the reservoir pressure, the drawdown pressure should be selected in such a way that the sand production rate is placed in the green area of the figure. This diagram becomes important when the reservoir pressure decreases to less than 3000 psi due to depletion. In that case, the low values of BHFP will increase the sand production rate beyond the permissible limit.

In addition, drawing the safe drawdown window and determining the critical drawdown pressure (safe drawdown line) is another unique application of this hybrid numerical model in the study of the sand production process. As mentioned earlier, with increasing reservoir depletion, increasing effective stresses, and decreasing rock strength, the amount of sand production in the wellbore also increases. So, the drawdown pressure in the wellbore should be selected in such a way that it leads to no production of sand or allowed amounts of sand production. Therefore, it is very important to prepare a CDDP diagram (safe drawdown window) for any reservoir that has unconsolidated sandstone. Figure 18 shows the outline of the safe drawdown window plot (Hussein and Ni 2018). In this figure, the diagram is divided into

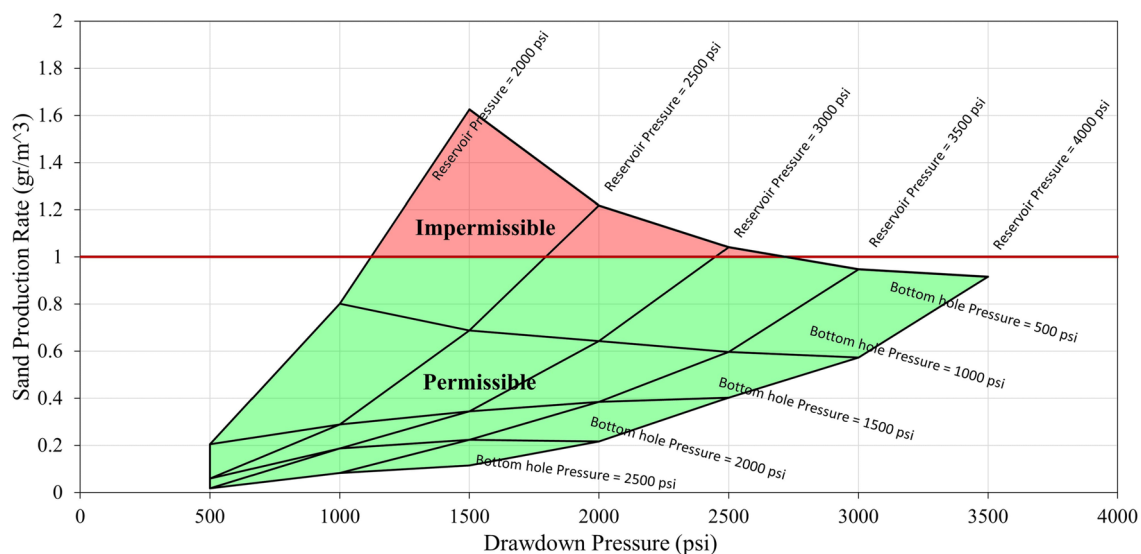


Fig. 17 Determination of the optimal drawdown pressure, according to the reservoir pressure and different values of the sand production rate in a vertical well with a daily flow rate of 2000 barrels in layer A10 of Asmari reservoir

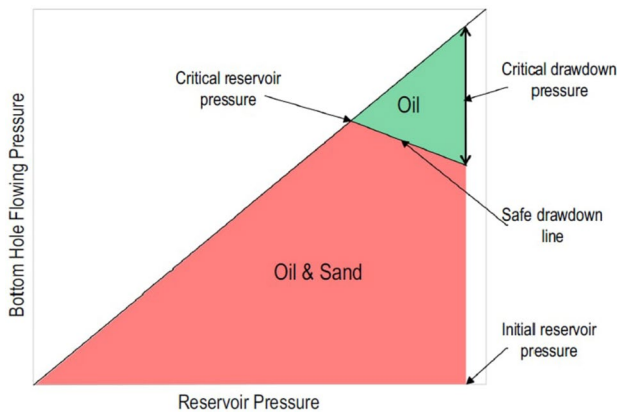


Fig. 18 Safe drawdown window to determine CDDP for sand production control (Hussein and Ni 2018)

Table 2 Critical drawdown pressure corresponds to the permissible limit of sand production for different reservoir pressures

Reservoir Pressure (psi)	Critical Draw-down Pressure (psi)
2000	1120
2500	1794
3000	2452

two parts. The white part is related to the situation where the bottom hole flowing pressure is higher than the reservoir pressure and technically, there will be no fluid production in this area. The colored area, which itself is divided into two colors, green and red, determines the value of the reservoir pressure corresponding to the BHFP. In other words, each point in this area shows the amount of pressure of the reservoir and the well according to the production of sand. If that point is in the red area, then the sand will be produced along with the fluid flow, and if the desired point is located in the green area, the fluid flow will be sand-free or in a permissible rate of sand production. The border between the green and red areas is called the safe drawdown line (Hussein and Ni 2018).

According to the curves in Fig. 15, the values of drawdown pressure corresponding to the points of the diagram where the sand production rate is equal to the permissible limit (1.0 g/m³), will be the CDDP of the wellbore. This means that the drawdown pressure above these values leads to the production of significant amounts of sand. The measured CDDP values along with the reservoir pressures corresponding to each value are listed in Table 2. Based on the values of reservoir pressure and CDDP, the value of critical BHFP is also calculated and in the next step, the diagram of BHFP vs. reservoir pressure is drawn (Fig. 19).

In Fig. 19, the red line of the diagram represents the safe drawdown line (according to the permissible rate of 1.0 g/

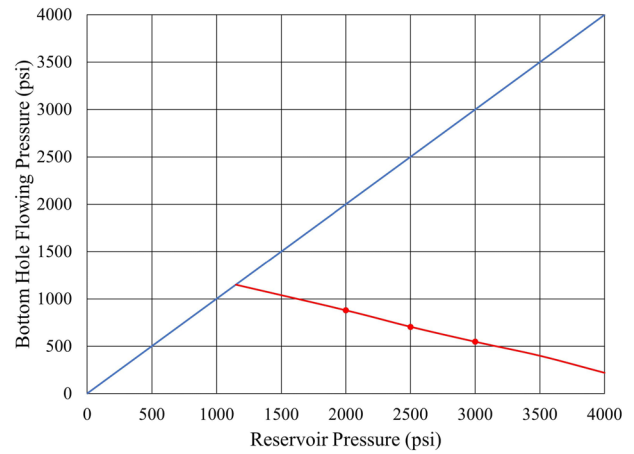


Fig. 19 Drawing the safe drawdown line for the vertical well located in layer A10 of the Asmari reservoir using the diagram in Fig. 15 and the data in Table 2

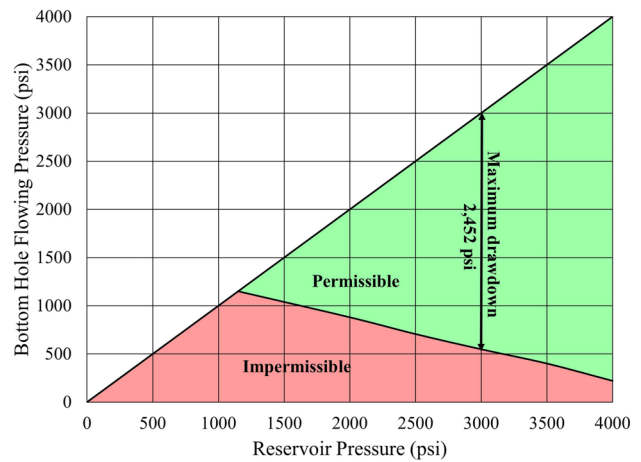


Fig. 20 Safe drawdown window for a vertical wellbore located in layer A10 of the Asmari reservoir (wellbore flow rate is 2000 bbl/day and permissible rate of sand production is 1.0 g/m³)

m³). In other words, each point above and below the safe drawdown line shows the permissible and impermissible rate of sand production, respectively. The descriptive form of this diagram can be seen in Fig. 20. According to the figure, if the reservoir pressure is 3,000 psi in this wellbore, the maximum drawdown pressure under which the fluid flow will produce sand at a permissible rate is 2452 psi. Also, for a reservoir pressure of 2000 psi, the maximum permissible drawdown pressure is 1120 psi.

However, as mentioned above, keeping the drawdown pressure within an allowable range does not necessarily keep the sand production rate stable for a long time. According to Figs. 15, 16 and 17, despite the drawdown pressure being constant at a certain value (for example, 1500 psi), with the increase in oil production or/and decrease in reservoir

pressure, the sand production rate will also increase. Instead, by keeping the BHFP constant in a certain range, despite the reduction in reservoir pressure, the sand production rate can be controlled for a longer period.

It should be noted that the permissible ranges shown in Figs. 17 and 20 are only related to a vertical well with a flow rate of 2,000 bbl/day and with a permissible sand production rate of 1.0 g/m^3 (green areas in the figures). That is, by increasing the flow rate to more than 2,000 bbl/day and by reducing the permissible rate of sand production to less than 1.0 g/m^3 , the green areas become smaller and the impermissible areas (red areas in the figures) become more extensive.

Determination of the safe drawdown window is very important in the exploitation of wells to reduce sand production in the long term and also in reservoir development plans. In this study, the safe drawdown window (or CDDP) in layer A10 of the Asmari reservoir has been determined only for vertical wells. Since the sand production rate changes according to the deviation angle of the well, therefore, separate numerical modeling is needed to measure the CDDP and the safe drawdown window in horizontal and deviated wells.

Based on the above, this hybrid numerical model can simulate and investigate the phenomenon of sand production practically and realistically in oil and gas wells, while the previous DEM models have mostly had a theoretical and study aspect. The model incorporates both the discontinuum structure of particles and the continuum spaces around them, along with several geomechanical parameters that play a crucial role in the sand production process. These features make the presented numerical modeling more accurately simulate the real conditions of the reservoir and the structure of the wellbore and perforations. Also, using this numerical modeling approach, it is possible to determine some of the optimal values such as direction of perforating, azimuth and deviation of the inclined wellbores, production flow rate, etc., which are effective in decreasing sand production rate. All these capabilities can reveal other aspects of the sand production process for researchers.

Although this developed model is a new method in studying the sand production process, it is obvious that it also has some shortcomings and limitations. For example, modeling with this method requires a large number of input parameters. In petroleum geomechanics, measuring and determining some of these parameters are very difficult and sometimes they are associated with errors and uncertainties. The time-consuming execution of calculations is another limitation of using this numerical model. Especially with the increase in the dimensions of the sanding zone and the subsequent increase in the number of modeled particles, the volume of calculations has also increased, which reduces the system's processing speed. Also, as the simulation becomes more complicated, it is necessary to run the program many

times to calibrate the model and perform sensitivity analysis. In this situation, to reduce the time of the analysis, supercomputers with powerful processors are needed.

To calibrate the numerical models with production conditions in oil fields, it is necessary to accurately determine the sand production rate in wells using sand monitoring tools such as intrusive or non-intrusive equipment. In this case, the results obtained from the models will be more reliable. Also, when calibrating numerical models related to a certain layer, to obtain more accurate results, it is necessary to construct models for some wells with different conditions. Then, after conducting a statistical study and averaging the results, the diagrams in Figs. 15 to 20 can be drawn more accurately. However, performing these analyses takes a lot of time. With the development of scripting and the use of other software facilities employed in this modeling, it becomes feasible to overcome some of the deficiencies and constraints of this simulation. This, in turn, can enable researchers to bridge the gaps in understanding the sand production phenomenon. It is worth mentioning that this modeling approach is not limited to simulating the sand production process. By modifying the model structure, it can be used to investigate other processes in petroleum geomechanics, such as wellbore stability, optimal mud pressure, casing collapse, hydraulic fracturing, and more. For example, by substituting a program based on a discrete element method (such as 3DEC) with the granular structure of PFC3D in this model, it is possible to simulate the process of hydraulic fracturing in oil wells.

Conclusions

In this article, a new FDM-DEM-FEM-CFD hybrid numerical model has been used to investigate the effect of drawdown pressure on the sand production rate, determine CDDP, and provide a safe drawdown window in layer A10 of the Asmari reservoir located in one of the oil fields in southwest Iran. For this purpose, the variation of sand production rate compared to different reservoir pressures for a vertical well with a constant BHFP was investigated. Then, by performing an extensive sensitivity analysis on different values of reservoir pressure and drawdown pressure, the values of sand production rate corresponding to each situation were measured. The results of the analysis carried out in this study can be listed as follows:

- While the reservoir pressure is constant, the sand production rate increases as the BHFP decreases.
- If the BHFP is constant, a gradual increase in the drawdown pressure will change the sand production rate up to a specific value. After that, the process of changes in the sand production rate will remain at a constant value.

- Increasing drawdown pressure for high values of BHFP (more than 1,500 psi), increases the sand production rate, and for low values of BHFP (less than 1,500 psi), decreases the sand production rate.
- Increasing drawdown pressure for low values of reservoir pressure (below 3,000 psi), increases the sand production rate, and for high values of reservoir pressure (above 3,000 psi), decreases the sand production rate.
- If the drawdown pressure is constant, the sand production rate will increase as the reservoir pressure decreases. Therefore, in the safe drawdown window, keeping the drawdown pressure constant in an acceptable range cannot necessarily keep the sand production rate stable for a long time at a permissible value.
- Despite the reservoir depletion due to continued production, keeping the BHFP constant in a certain range will control sand production at a permissible rate for a longer period.
- The numerical model presented in this study can investigate the variations in the sand production rate due to the drawdown pressure changes and also determine the CDDP for sand control with acceptable precision.

Acknowledgements The authors wish to acknowledge the National Iranian South Oil Company (NISOC) for providing support in conducting this research.

Declarations

Conflict of interest The authors have no conflicts of interest to declare that are relevant to the content of this article.

Ethical approval All procedures performed in studies involving human participants were in accordance with the ethical standards of the institutional and/or national research committee and with the 1964 Helsinki declaration and its later amendments or comparable ethical standards.

Informed consent Informed consent was obtained from all individual participants included in the study.

Open Access This article is licensed under a Creative Commons Attribution 4.0 International License, which permits use, sharing, adaptation, distribution and reproduction in any medium or format, as long as you give appropriate credit to the original author(s) and the source, provide a link to the Creative Commons licence, and indicate if changes were made. The images or other third party material in this article are included in the article's Creative Commons licence, unless indicated otherwise in a credit line to the material. If material is not included in the article's Creative Commons licence and your intended use is not permitted by statutory regulation or exceeds the permitted use, you will need to obtain permission directly from the copyright holder. To view a copy of this licence, visit <http://creativecommons.org/licenses/by/4.0/>.

References

- Abdollahie Fard I, Braathen A, Mokhtari M, Alavi SA (2006) Interaction of the Zagros fold thrust belt and the Arabian-type, deep-seated folds in the Abadan Plain and the Dezful Embayment, SW Iran. *Pet Geosci* 12:347–362. <https://doi.org/10.1144/1354-079305-706>
- Alavi M (2004) Regional stratigraphy of the Zagros fold-thrust belt of Iran and its proforeland evolution. *Am J Sci* 304:1–20. <https://doi.org/10.2475/ajs.304.1.1>
- Almedeij JH, Algharaib MK (2005) Influence of sand production on pressure drawdown in horizontal wells: theoretical evidence. *J Pet Sci Eng* 47:137–145. <https://doi.org/10.1016/j.petrol.2005.03.005>
- Berberian M (1995) Master “blind” thrust faults hidden under the Zagros folds: active basement tectonics and surface morphotectonics. *Tectonophysics* 241:193–224. [https://doi.org/10.1016/0040-1951\(94\)00185-C](https://doi.org/10.1016/0040-1951(94)00185-C)
- Climent N, Arroyo M, O’Sullivan C, Gens A (2013) Sensitivity to damping in sand production DEM-CFD coupled simulations. *AIP Conf Proc* 1542:1170–1173. <https://doi.org/10.1063/1.4812145>
- Climent N, Arroyo M, O’Sullivan C, Gens A (2014) Sand production simulation coupling DEM with CFD. *Eur J Environ Civ Eng* 18(9):983–1008. <https://doi.org/10.1080/19648189.2014.920280>
- Cui Y, Nouri A, Chan D, Rahmati E (2016) A new approach to DEM simulation of sand production. *J Pet Sci Eng* 147:56–67. <https://doi.org/10.1016/j.petrol.2016.05.007>
- Detournay, C (2008) Numerical modeling of the slit mode of cavity evolution associated with sand production. Society of Petroleum Engineers Inc., SPE 116168, pp 1–10. <https://doi.org/10.2118/116168-MS>
- Dung TQ, Tung HT (2014) The model to predict sand production for production wells at Cuu Long basin. *Sci Technol Dev* 17(K5):1–7. <https://doi.org/10.32508/stdj.v17i3.1493>
- Eshiet K, Sheng Y (2013) Influence of rock failure behaviour on predictions in sand production problems. *Environ Earth Sci* 70:1339–1365. <https://doi.org/10.1007/s12665-013-2219-0>
- Eshiet KI, Yang D, Sheng Y (2019) Computational study of reservoir sand production mechanisms. *Geotech Res* 6(3):177–204. <https://doi.org/10.1680/jgere.18.00026>
- Fjær E, Holt RM, Horsrud P, Raaen AM, Risnes R (2008) *Petroleum related rock mechanics*, vol 53, 2nd edn. Elsevier, Amsterdam
- Ghalambor A, Hayatdavoudi A, Alcocer CF, Koliba RJ (1989) Predicting sand production in U.S. Gulf Coast gas wells producing free water. Society of Petroleum Engineers Inc., pp 1336–1343. <https://doi.org/10.2118/17147-PA>
- Ghalambor A, Hayatdavoudi A, Koliba RJ (1994) A study of sensitivity of relevant parameters to predict sand production. Society of Petroleum Engineers Inc., SPE 27011, pp 883–895. <https://doi.org/10.2118/27011-MS>
- Gwamba G, Changyin D, Bo Z (2022) Investigating unary, binary and ternary interactive effects on pressure drawdown for optimal sand production prediction. *J Pet Sci Eng* 218:1–14. <https://doi.org/10.1016/j.petrol.2022.111010>
- Hansen B (2018) Production casing design considerations. Devon Energy Corporation (NYSE: DVN). www.devonenergy.com
- Hussein AM, Ni Q (2018) Numerical modeling of onset and rate of sand production in perforated wells. *J Pet Explor Prod Technol* 8:1255–1271. <https://doi.org/10.1007/s13202-018-0443-6>
- Itasca Consulting Group, Inc. (2019) PFC3D (Particle flow code in 3 dimensions)—user’s manual. Version 6.00.13. <https://www.itascacg.com/software/pfc>. Minneapolis, Minnesota USA
- Itasca Consulting Group, Inc. (2021) FLAC3D (Fast Lagrangian analysis of continua in 3 dimensions)—user’s manual. Version 7.0. <https://www.itascacg.com/software/flac3d>. Minneapolis, Minnesota USA
- Issa MA, Hadi FA, Nygaard R (2022) Coupled reservoir geomechanics with sand production to minimize the sanding risks in unconsolidated reservoirs. *Pet Sci Technol* 40(9):1065–1083. <https://doi.org/10.1080/10916466.2021.2014522>

- Kasim, A, Wijnands F, Subbiah S (2008) Bokor – a new look at sand production in a mature field. *SPE Drilling & Completion*, pp 415–423. <https://doi.org/10.2118/102242-PA>
- Kessler, N, Wang Y, Santarelli FJ (1993) A simplified pseudo 3D model to evaluate sand production risk in deviated cased holes. *Society of Petroleum Engineers, Inc.*, pp 323–332. <https://doi.org/10.2118/26541-MS>
- Li X, Feng Y, Gray KE (2018) A hydro-mechanical sand erosion model for sand production simulation. *J Pet Sci Eng* 166:208–224. <https://doi.org/10.1016/j.petrol.2018.03.042>
- Lu Y, Xue C, Liu T, Chi M, Yu J, Gao H, Xu X, Li H, Zhuo Y (2021) Predicting the critical drawdown pressure of sanding onset for perforated wells in ultra-deep reservoirs with high temperature and high pressure. *Energy Sci Eng* 9(9):1517–1529. <https://doi.org/10.1002/ese3.922>
- Morita N, Whitfill DL, Massie I, Knudsen TW (1989a) Realistic sand-production prediction: numerical approach. *Society of Petroleum Engineers Inc.*, pp 15–24. <https://doi.org/10.2118/16989-PA>
- Morita N, Whitfill DL, Fedde OP, Levik TH (1989b) Parametric study of sand-production prediction: analytical approach. *Society of Petroleum Engineers Inc.*, pp 25–33. <https://doi.org/10.2118/16990-PA>
- Nguyen VH, Bui TTL (2021) Geomechanical model and sanding onset assessment: a field case study in Vietnam. *Petrovietnam J* 10:40–46. <https://doi.org/10.47800/PVJ.2021.10-04>
- Nouri A, Vaziri H, Kuru E, Islam R (2006a) A comparison of two sanding criteria in physical and numerical modeling of sand production. *J Pet Sci Eng* 50:55–70. <https://doi.org/10.1016/j.petrol.2005.10.003>
- Nouri A, Vaziri H, Belhaj H, Islam R (2003) A comprehensive approach to modeling sanding during oil production. *Society of Petroleum Engineers Inc.*, SPE 81032, pp 1–7. <https://doi.org/10.2118/81032-MS>
- Nouri A, Vaziri H, Kuru E, Islam R (2006b) Sand-production prediction: a new set of criteria for modeling based on large-scale transient experiments and numerical investigation. *Society of Petroleum Engineers Inc.*, pp 227–237. <https://doi.org/10.2118/90273-PA>
- Oladoyin K, Gabriella FK, István S (2018) Formation Susceptibility to Wellbore Instability and Sand Production in the Pannonian Basin, Hungary. *American Rock Mechanics Association (ARMA)*
- Papamichos E, Stavropoulou M (1998) An erosion-mechanical model for sand production rate prediction. *Int J Rock Mech Min Sci* 35:531–532. [https://doi.org/10.1016/S0148-9062\(98\)00106-5](https://doi.org/10.1016/S0148-9062(98)00106-5)
- Papamichos E, Vardoulakis I, Tronvoll J, Skjvrstein A (2001) Volumetric sand production model and experiment. *Int J Numer Anal Meth Geomech* 25:789–808. <https://doi.org/10.1002/nag.154>
- Pham ST (2017) Estimation of sand production rate using geomechanical and hydromechanical models. *Adv Mater Sci Eng* 9:1–11. <https://doi.org/10.1155/2017/2195404>
- Potyondy DO, Mas Ivars D (2020) Simulating spalling with a flat-jointed material. *Appl Numer Model Geomech* 1–5
- Potyondy DO, Cundall PA (2004) A bonded-particle model for rock. *Int J Rock Mech Min Sci* 41:1329–1364. <https://doi.org/10.1016/j.ijrmms.2004.09.011>
- Potyondy DO, Vatcher J, Emam S (2020) Modeling of spalling with PFC3D: a quantitative assessment (612):371–4711. *Itasca Consulting Group, Minneapolis, Minnesota USA*
- Potyondy DO (2018) A flat-jointed bonded-particle model for rock. *American Rock Mechanics Association (ARMA)*, 1–12
- Potyondy DO (2019) Material-modeling support in PFC [fistPkg6.6] (Example materials 1). *Itasca Consulting Group (Memorandum)*, Minneapolis, Minnesota USA
- Rahman MM, Rahman MK (2012) Optimizing hydraulic fracture to manage sand production by predicting critical drawdown pressure in gas well. *J Energy Resour Technol* 134(1):013101-1–013101-9. <https://doi.org/10.1115/1.4005239>
- Ramos GC, Katahara KW, Gray JD, Knox DJW (1999) Sand production in vertical and horizontal wells in a friable sandstone formation, North Sea. *Society of Petroleum Engineers Inc.*, SPE 28065, pp 309–315. <https://doi.org/10.2118/28065-MS>
- Risnes R, Bratli RK, Horsrud P (1982) Sand stresses around a wellbore. *Soc Pet Eng AIME* 22(6):883–898. <https://doi.org/10.2118/9650-PA>
- API Specification, 5CT (2012) ISO 11960:2011 Petroleum and natural gas industries—steel pipes for use as casing or tubing for wells. *American Petroleum Institute (Purchasing Guidelines)*
- Subbiah SK, de Groot L, Graven H (2014) An innovative approach for sand management with downhole validation. *Society of Petroleum Engineers (SPE)*, pp 1–15. <https://doi.org/10.2118/168178-MS>
- Sun Z, Liu H, Han Y, Basri MA, Mesdour R (2021) The optimum pressure drawdown for production from a shale gas reservoir: a numerical study with a coupled geomechanics and reservoir model. *J Nat Gas Sci Eng* 88(103848):1–9. <https://doi.org/10.1016/j.jngse.2021.103848>
- Tsuji Y, Kawaguchi T, Tanaka T (1993) Discrete particle simulation of two-dimensional fluidized bed. *Powder Technol* 77(1):79–87. [https://doi.org/10.1016/0032-5910\(93\)85010-7](https://doi.org/10.1016/0032-5910(93)85010-7)
- Vásquez AR, Sánchez MS, Yáñez RL, Poquioma W, El Chirity K (1999) The diagnosis, well damage evaluation and critical drawdown calculations of sand production problems in the Ceuta Field, Lake Maracaibo, Venezuela. *Society of Petroleum Engineers Inc.*, SPE 54011, pp 1–11. <https://doi.org/10.2118/54011-MS>
- Vaziri H, Barree B, Xiao Y, Palmer I, Kutas M (2002) What is the magic of water in producing sand. *Society of Petroleum Engineers Inc.*, SPE 77683, pp 1–13. <https://doi.org/10.2118/77683-MS>
- Vaziri H, Nouri A, Hovem K, Wang X (2008) Computation of sand production in water injectors. *Society of Petroleum Engineers Inc.*, pp 518–524. <https://doi.org/10.2118/107695-PA>
- Veeken CAM, Davies DR, Kanter CJ, Kooijman AP (1991) Sand production prediction review: developing an integrated approach. *Society of Petroleum Engineers Inc. (SPE)*, pp 1–12. <https://doi.org/10.2118/22792-MS>
- Weingarten JS, Perkins TK (1995) Prediction of sand production in gas wells: methods and Gulf of Mexico Case Studies. *Society of Petroleum Engineers Inc.*, pp 596–600. <https://doi.org/10.2118/24797-PA>
- Willson SM, Moschovidis ZA, Cameron JR, Palmer ID (2002) New model for predicting the rate of sand production. *Society of Petroleum Engineers Inc. (SPE)*, pp 1–9. <https://doi.org/10.2118/78168-MS>
- Yosif TK, Al-Sudani JA (2022) Geomechanical study to predict the onset of sand production formation. *J Eng* 28:1–17. <https://doi.org/10.31026/j.eng.2022.02.01>
- Younessi A, Rasouli V, Wu B (2013) Sand production simulation under true-triaxial stress conditions. *Int J Rock Mech Min Sci* 61:130–140. <https://doi.org/10.1016/j.ijrmms.2013.03.001>
- Zalakinezhad A, Jamshidi S (2021) Numerical modeling of the amount and rate of sand produced in oil wells. *J Pet Sci Technol* 11(3):33–43. <https://doi.org/10.22078/jpst.2022.4679.1771>
- Zhang R, Shi X, Zhu R, Zhang C, Fang M, Bo K, Feng J (2016) Critical drawdown pressure of sanding onset for offshore depleted and water cut gas reservoirs: modeling and application. *J Nat Gas Sci Eng* 34:159–169. <https://doi.org/10.1016/j.jngse.2016.06.057>

Publisher's Note Springer Nature remains neutral with regard to jurisdictional claims in published maps and institutional affiliations.